5 Nanomechanics of Aggrecan: A New Perspective on Cartilage Biomechanics, Disease and Regeneration

Chao Wang, Elizabeth R. Kahle, Qing Li, and Lin Han

Abstract

Articular cartilage is a hydrated macromolecular composite mainly composed of type II collagen fibrils and the large proteoglycan, aggrecan. Aggrecan is a key determinant of the load bearing and energy dissipation functions of cartilage. Previously, studies of cartilage biomechanics have been primarily focusing on the macroscopic, tissue-level properties, which failed to elucidate the molecular-level activities that govern cartilage development, function, and disease. This chapter provides a brief summary of Dr. Alan J. Grodzinsky's seminal contribution to the understanding of aggrecan molecular mechanics at the nanoscopic level. By developing and applying a series of atomic force microscopy (AFM)-based nanomechanical tools, Grodzinsky and colleagues revealed the unique structural and mechanical characteristics of aggrecan at unprecedented resolutions. In this body of work, the "bottle-brush"-like ultrastructure of aggrecan was directly visualized for the first time. Meanwhile, molecular mechanics of aggrecan was studied using a physiological-like 2D biomimetic assembly of aggrecan on multiple fronts, including compression, dynamic loading, shear, and adhesion. These studies not only generated new insights into the development, aging, and disease of cartilage, but established a foundation for designing and evaluating novel cartilage regeneration strategies. For example, building on the scientific foundation and methodology infrastructure established by Dr. Grodzinsky, recent studies have elucidated the roles of other proteoglycans in mediating cartilage integrity, such as decorin and perlecan, and evaluated the therapeutic potential of biomimetic proteoglycans in improving cartilage regeneration.

Keywords

Proteoglycan · Nanomechanics · AFM · Aggrecan · Decorin

5.1 Introduction

Articular cartilage is the soft tissue at the end of bones that enables joint locomotion, energy dissipation, and lubrication [40]. These functions are endowed by the specialized extracellular matrix (ECM) of cartilage, a hydrated composite of col-

C. Wang · E. R. Kahle · Q. Li · L. Han (✉)
School of Biomedical Engineering, Science and Health Systems, Drexel University, Philadelphia, PA, USA
e-mail: lh535@drexel.edu

B. K. Connizzo et al. (eds.), *Electromechanobiology of Cartilage and Osteoarthritis*, Advances in Experimental Medicine and Biology 1402, https://doi.org/10.1007/978-3-031-25588-5_5

lagens and proteoglycans that are synthesized by residing chondrocytes [26] (Fig. 5.1a). Osteoarthritis (OA), the most prevalent musculoskeletal disease, is characterized by the irreversible breakdown of cartilage ECM, resulting in severe joint pain and limited motion [45]. Due to its avascular and dense nature, cartilage has very limited self-repair capabilities, and regenerative therapies often fail to restore the structure and function of healthy tissue [29]. This renders it crucial to understand the establishment, homeostasis, and disease-induced degeneration of cartilage ECM. The ECM mainly consists of ~65–70% w/w water, ~20–30% collagens, ~5–10% proteoglycans [40] as well as DNAs and other minor proteins/proteoglycans (Fig. 5.1a–c) [28]. *In vivo*, the collagen network is primarily responsible for cartilage tensile stiffness, while aggrecan and its negative fixed charges are the key determinants of cartilage compressive resistance and fluid flow-associated energy dissipative properties [40].

In the past few decades, there have been many attempts in understanding cartilage biomechanics in health and disease, in the hope to gain new insights into disease progression and functional regeneration. In the 1980's, Mow and colleagues applied the biphasic poroelasticity theory [2] to interpret the time-dependent, energy dissipative properties of cartilage. This theory addressed the key role of molecular friction arising from water-solid matrix interactions during fluid flow in contributing to energy dissipation [42]. Grodzinsky and colleagues further integrated the concept of electrical streaming potential with cartilage mechanical deformation and underscored the crucial role of fixed charges in overt tissue biomechanics [16, 17]. These seminal studies established the foundation of modern cartilage biomechanics theory. At the same time, numerous experimental tools have been implemented to delineate the contributions of each matrix constituent to cartilage mechanical properties, including confined and unconfined compression, indentation, dynamic oscillatory loading, and shear [39]. For instance, investigating the biomechanics of normal and glycosaminoglycan (GAG)-depleted cartilage have shown that aggrecan and its fixed charges directly contribute to ~50% compressive modulus of cartilage [60].

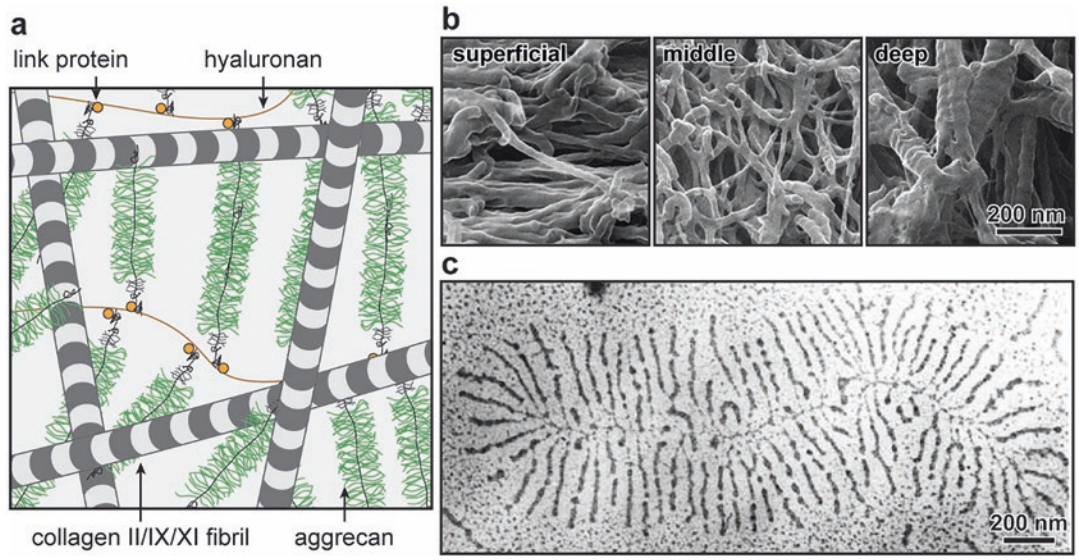

Fig. 5.1 An overview of articular cartilage extracellular matrix (ECM). (**a**) Schematic illustration of the major constituents in cartilage ECM: type II/IX/XI collagen fibril network and aggrecan-hyaluronan (HA) aggregates. (**b**) Depth-dependent nanostructure of collagen fibril network visualized by helium ion microscopy on proteoglycan-removed rabbit cartilage. Adapted with permission from Ref. [56]. (**c**) Nanostructure of aggrecan-HA aggregates imaged by transmission electron microscopy. (Adapted with permission from Ref. [3])

Despite these advances in tissue-level studies, disease intervention and regeneration remain elusive. This is at least partly because the tissue-level investigatory approaches are unable to account for the salient heterogeneity and a high level of complexity of cartilage structural hierarchy from nm-to-mm scales. For example, the collagen network is dominated by types II/IX/XI collagen heterotypic fibrils [15], with a minor amount of type III collagen co-assembling on the surface of collagen II fibrils [58]. The collagen fibrils (diameter ~ 30–80 nm) vary in orientation and diameter with depth in the tissue [9], from being transverse in the superficial layer, to random in the middle layer, then predominantly perpendicular in the deep layer, accompanied by an increasing gradient of fibril diameter and proteoglycan concentration (Fig. 5.1b) [56]. Aggrecan, the major proteoglycan, has a "bottle-brush" structure, and is decorated with highly negatively charged chondroitin sulfate (CS) and keratan sulfate (KS) GAGs along its core protein [26]. *In vivo*, aggrecan is end-attached to the linear hyaluronan (HA) molecules via its G1 domain at the N-terminal [27], and this interaction is further stabilized by link protein [4]. In the ECM, these supramolecular aggregates are entrapped within ~100 nm nanopores between collagen fibrils at ~50% molecular compressive strain [59], thereby adopting a highly compacted configuration that endows the tissue with its high fixed charge density and osmotic swelling pressure. The electron microscopy study by Buckwalter and Rosenberg highlighted the complexity in the assembly and retention of aggrecan *in vivo*, and provided the first direct visual evidence of the aggrecan-HA aggregation (Fig. 5.1c) [3]. Given these complexities, understanding the ECM from the molecular level is necessary for developing effective disease intervention and tissue regeneration.

Dr. Grodzinsky is the pioneer in studying the molecular mechanics of cartilage ECM constituents. Through collaboration with Dr. Christine Ortiz, a world-renowned scientist in polymer nanomechanics and atomic force microscopy, this team has made numerous transformative discoveries on the nanostructure and nanomechanics of cartilage, with a focus on the major proteoglycan, aggrecan. This chapter provides a brief summary of Grodzinsky's contributions to the understanding of aggrecan within the context of cartilage function, disease, and regeneration. This chapter begins with the summary of the ultrastructural and nanomechanical studies of native aggrecan (Sect. 5.2), followed by the overview of applying the knowledge of aggrecan to understanding cartilage aging, disease and tissue engineering (Sect. 5.3), and then, the discussion of more recent studies on other native and biomimetic proteoglycans that were directly inspired by the Grodzinsky's work (Sect. 5.4), and finally, concludes with a summary and future outlook (Sect. 5.5).

5.2 Ultrastructure and Nanomechanics of Aggrecan

One seminal contribution by Grodzinsky and colleagues is the direct visualization of the ultrastructure of aggrecan and its GAG side chains, which was the first of its kind [43]. In this study, Ng et al. deposited aggrecan molecules extracted from fetal epiphyseal and mature nasal bovine cartilage samples onto 3-aminopropyltriethoxysilane (APTES)-treated, positively charged, atomisticly flat mica surfaces. The nanostructure of aggrecan was then revealed via tapping mode AFM-imaging at a spatial resolution of ~2 nm. Imaging aggrecan at such unprecedented resolution enabled not only visualization of its "bottle-brush"-like molecular architecture, but also direct quantification of its structural parameters (Fig. 5.2a). This includes the core protein contour length, L_c, end-to-end distance, R_{ee}, degree of extension, R_{ee}/L_c, and the packing density and length of GAG bristles. In turn, the persistence length, L_p, as calculated from the worm-like chain model (~110 nm for fetal epiphyseal aggrecan), illustrated the highly extended conformation of aggrecan in its equilibrium state. Conversely, this study also showed that *in vivo*, aggrecan adapted a highly compacted conformation, for that the *in vivo* concentration is at least 40× higher than the densely packed form imaged on mica (Fig. 5.2b). To this end, the contrast

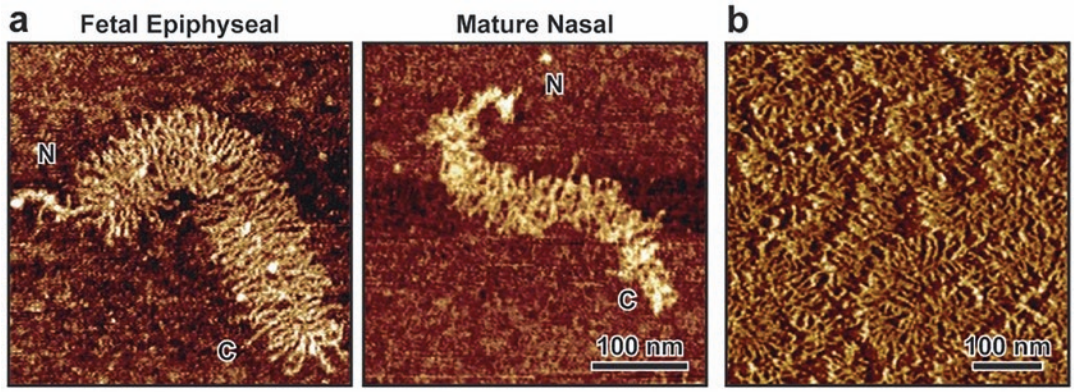

Fig. 5.2 Ultrastructure of aggrecan via tapping mode atomic force microscopy (AFM) imaging. (**a**) Nanostructure of individual fetal bovine epiphyseal and mature bovine nasal aggrecan deposited on atomicly flat mica surface. (**b**) Nanostructure of densely packed fetal bovine epiphyseal aggrecan monomers, illustrating the highly compressed conformation of aggrecan *in vivo* (~ 40× higher than the aggrecan packing imaged here). (Panels (**a**) and (**b**) are adapted with permission from Ref. [43])

between aggrecan from fetal epiphyseal versus mature nasal cartilage highlighted the large variation of its ultrastructure with tissue source and age (Fig. 5.2a). Furthermore, these high resolution images clearly illustrated the dominating role of longer CS-GAGs in contributing to the molecular conformation of aggrecan. Indeed, a follow-up study by Lee et al. compared the structure and conformation of aggrecan from a 29-year-old human donor subjected to chondroitinase ABC and keratanase II treatment, and confirmed that the extension and conformation of aggrecan is predominantly governed by the longer CS-GAGs, rather than the shorter KS-GAG chains [36].

In addition to nanostructure, Grodzinsky and colleagues also, for the first time, assessed the nanomechanics of aggrecan under multiple deformation modes, including compression, energy dissipation, shear, and adhesion. Building on earlier work of CS-GAG nanomechanics [51–53], Dean et al. chemically functionalized aggrecan with thiol-groups at its N-terminal, and end-attached thiol-functionalized aggrecan onto gold-coated planar silicon substrates and microspherical AFM colloidal tips ($R \approx 2.5$ μm). This set-up established a 2D biomimicry assembly of aggrecan at ~50 mg/mL, near its physiological packing density (~20–80 mg/mL), thus enabling the studies of aggrecan interactions under *in vivo*-like conditions. With this biomimetic system, the team performed an in-depth analysis of key molecular mechanical behaviors of aggrecan. First, compressive nanomechanics was quantified using force spectroscopy and contact mode AFM imaging in aqueous solutions with varied ionic strength (IS) conditions [10, 11]. As expected, the long-range repulsion force between two opposing aggrecan layers extended to >1 μm in IS = 0.001 M solution, while the distance and magnitude of compression resistance decreased drastically with increasing IS from 0.001 to 1.0 M (Fig. 5.3a). Applying Poisson-Boltzmann-based models, this study confirmed that the electrical double layer (EDL) repulsion interactions arising from CS-GAGs play a dominating role in the compressive nanomechanics of aggrecan, in comparison to other non-electrostatic factors such as steric hindrance and conformational entropy. Importantly, under *in vivo* conditions (IS = 0.15 M), given that the Debye length, $\kappa^{-1} \approx 0.8$ nm, is at the same order of GAG-GAG packing distance (~ 2–3 nm), the salient heterogeneity in electrical potential was a key factor in determining the magnitude of repulsion. While the continuum Donnan model substantially overestimated the repulsion force, both the unit cell model [5] and charged rod model [12], which accounted for the nanoscale spatial heterogeneity of electrical potential, accurately predicted the aggrecan-aggrecan repulsion [10].

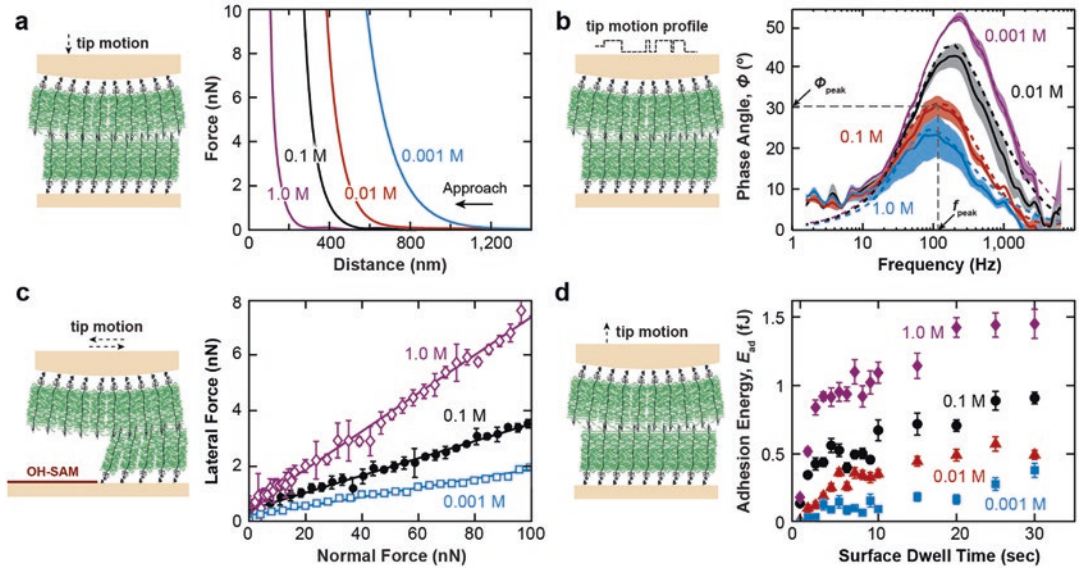

Fig. 5.3 Nanomechanics of aggrecan measured between two opposing layers of aggrecan via atomic force microscopy (AFM)-based nanomechanical modalities. Experiments were performed applying aggrecan functionalized colloidal tips ($R \approx 2.5$ μm, except that $R \approx 22.5$ μm for panel (**b**) to aggrecan-functionalized planar substrates in NaCl aqueous solutions at different ionic strengths (IS = 0.001–1.0 M). Left panels: Schematics of experimental set-ups. For panel (**c**), the substrate was prepared via micro-contact printing to form micropatterned surface of hydroxyl-terminated self-assembled monolayer (OH-SAM, $HS(CH_2)_{11}OH$) and aggrecan monolayer. Right panels: (**a**) Compressive force-versus distance curves as a function of bath IS via colloidal molecular force spectroscopy. Adapted with permission from Ref. [10]. (**b**) The magnitude of phase angle, ϕ, of newborn human aggrecan as a function of dynamic frequency and bath IS via AFM-based nanorheometric test (mean ± 95% CI, $n = 6$). Adapted with permission from Ref. [44]. (**c**) Lateral versus applied normal force curves as a function of bath IS via lateral force microscopy (mean ± SD, $n = 8$). Adapted with permission from Ref. [24]. (**d**) The total aggrecan-aggrecan adhesion energy as a function of surface dwell time and bath IS via molecular force spectroscopy (mean ± SEM, $n \geq 30$). (Adapted with permission from Ref. [23])

Following the studies of elasticity, Nia et al. probed the energy dissipative, poroelastic nanomechanics of aggrecan using the custom-built AFM-nanorheometer [44]. Similar to the case of elastic modulus, the energy dissipation of aggrecan layer is also largely governed by the EDL repulsion, as illustrated by the salient dependence of phase angle on bath IS (Fig. 5.3b). Meanwhile, the dynamic oscillatory loading responses of three specimens were compared: normal cartilage, GAG-depleted cartilage, and the end-attached aggrecan monolayers. In the low frequency elastic domain, the modulus of GAG-depleted cartilage, E_L, was ~1.5 × lower than that of the normal cartilage, while the modulus of aggrecan layer is ~7 × lower. Despite this much lower modulus, the aggrecan monolayer had comparable hydraulic permeability, k, to the native cartilage, while that of the GAG-depleted cartilage was ~24 × higher. Such contrast underscored the direct contribution of aggrecan and its sGAGs to cartilage fluid flow and pressurization capabilities. This is because the closely spaced GAG chains of aggrecan, with an effective pore size ~2–4 nm, provide the main resistance to intra-tissue fluid flow in cartilage, as manifested in the GAG-GAG nanomolecular model of hydraulic permeability [14], while the collagen network has a much larger pore size (~100 nm), resulting in elevated hydraulic permeability. Similar to the case of elasticity, a more complex structural model was needed to capture the magnitude of aggrecan-endowed energy dissipation. The fiber-reinforced model [55] or transversely isotropic model [54], which accounted for cartilage tension-compression asymmetry, were able

to quantitatively capture the degree of energy dissipation, while an isotropic poroelastic model would markedly underestimate these values.

Applying lateral force microscopy (LFM), Han et al. elucidated the shear nanomechanics of both single and two opposing aggrecan layers [24, 25]. The shear resistance of aggrecan was quantified as a function of aggrecan layer height and applied normal force under varied IS. The lateral linearity ratio, μ (= $dF_{lateral}/dF_{normal}$), was found to vary significantly with both IS (Fig. 5.3c) and lateral displacement rate, suggesting that the shear resistance was also largely governed by both EDL repulsion and fluid flow. At lower IS, given the dominance of EDL repulsion, aggrecan exhibited a more extended conformation. Therefore, a lower lateral proportional coefficient could be attributed to the minimal interdigitation between opposing aggrecan and strong water hydration effects surrounding negative charges, similar to the highly lubricative case of negatively charged synthetic polyelectrolytes. To this end, the shear of two opposing aggrecan layers also yielded a lower lateral coefficient, due to stronger EDL repulsion than just one single layer. In addition, divalent Ca^{2+} ions (~2–4 mM in cartilage [40]) were also found to mediate the shear behavior through extra screening of EDL repulsion and potentially the ion bridging effect. Collectively, EDL repulsion dominates not only the compressive, but also shear nanomechanics of aggrecan. It is also worth noting that the low lateral coefficient, μ, observed here does not imply a role of aggrecan in cartilage lubrication, as the concentration of aggrecan on cartilage surface is very low, and the synovial fluid is dominated by fragmented aggrecan, which lacks the G1-domain that enables its binding to HA [50].

Interestingly, despite the dominance of strong EDL repulsion, aggrecan also exhibited marked adhesive interactions with adjacent aggrecan molecules [23], and with collagen II fibrils [49]. When compressed at physiological-like molecular strain (~50% [59]) for 0–30 seconds, aggrecan was found to undergo pronounced adhesion, with a magnitude at ~1 pN between per pair of aggrecan-aggrecan, and ~ 0.3 pN per aggrecan molecule versus collagen II fibrils in physiological-like solution. Such adhesion was attributed to non-specific interactions, such as hydrogen bonding, hydrophobicity, ionic interactions as well as physical entanglement. Increasing EDL repulsion by lowering IS effectively limited the intermolecular contact and reduced the adhesion between the layers (Fig. 5.3d). On the other hand, Ca^{2+}-mediated ion bridging further enhanced the adhesion by providing additional ionic linkage. Given that the highly compressed state of aggrecan mimics the physiological molecular strain in unloaded cartilage, these non-specific interactions were hypothesized to be an important biophysical factor that helps stabilizing the retention of fragmented aggrecan in healthy cartilage and contributes to the integrity of cartilage ECM.

5.3 Implications for Aging, Disease and Regeneration

Following these fundamental studies of aggrecan, Grodzinsky and colleagues further applied the experimental paradigm to gain new molecular insights into cartilage disease pathogenesis and regenerative medicine. One important application was to assess age-associated changes of aggrecan polymorphism using human cartilage samples. Applying tapping mode AFM imaging and force spectroscopy, Lee et al. compared aggrecan molecules from newborn and 38-year-old adult donors [36]. Aggrecan from newborn cartilage exhibited superior nanostructure and compressive nanomechanics relative to that from adult cartilage. First, the adult aggrecan population consisted of substantially more fragmented monomers that did not have the G1 or G3 globular domain (Fig. 5.4a, left panel). Such observation illustrated that aggrecan fragmentation could be a normal homeostasis process during growth and aging, and is a prevalent feature even in healthy adult cartilage. It also indicated that the retention of aggrecan *in vivo* may require additional mechanisms beyond the aggrecan-HA association, such as the aggrecan-aggrecan and aggrecan-collagen II adhesion [23, 49]. And, even for the sub-population of full length aggre-

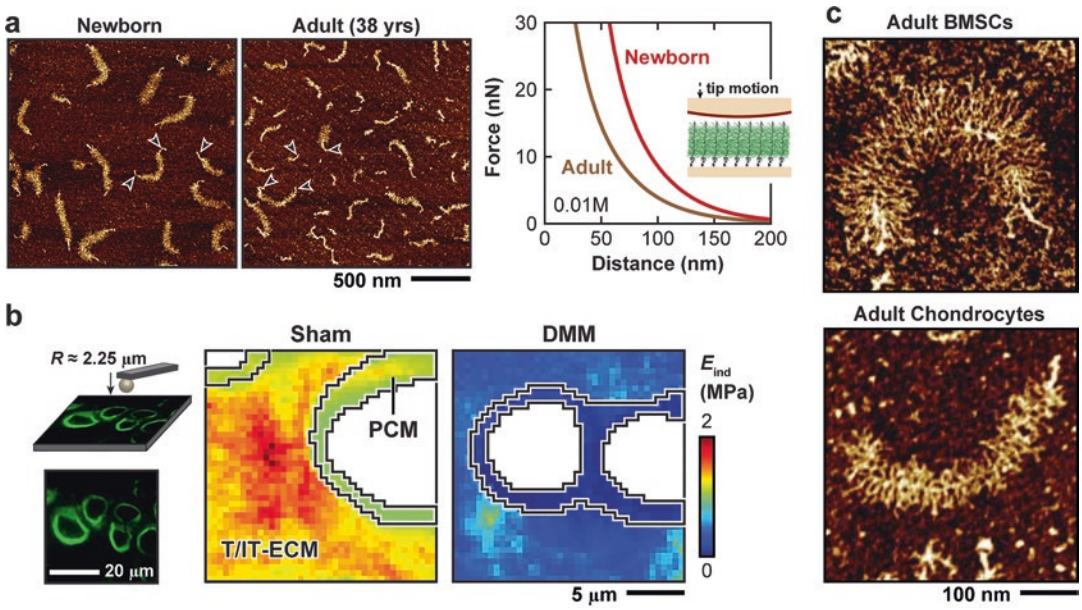

Fig. 5.4 Applications of AFM in the studies of aggrecan in cartilage aging, disease initiation and tissue engineering. (**a**) Left panel: Tapping mode AFM height images of newborn and adult (38-year-old) human aggrecan monomers. Arrow heads: globular domains. Right Panel: Compression resistance curves of end-attached newborn and adult human aggrecan monolayer measured at 0.01 M ionic strength via colloidal force spectroscopy. (Adapted with permission from Ref. [36]). (**b**) Left panel: Schematic illustration of immunofluorescence (IF)-guided AFM nanomechanical mapping on mature murine cartilage cryosection using a microspherical colloidal tip; the pericellular matrix (PCM) is immunolabeled with collagen VI. Right panel: Representative indentation modulus maps show the early reduction of PCM and territorial/inter-territorial extracellular matrix (T/IT-ECM) modulus at 1 week after applying the destabilization of the medial meniscus (DMM) surgery to 3-month-old male wild-type mice, relative to the Sham control. (Adapted with permission from Ref. [6]). (**c**) Tapping mode AFM height images of aggrecan ultrastructure synthesized by adult equine bone marrow stromal cells (BMSCs) and chondrocytes. (Adapted with permission from Ref. [33])

can, the newborn aggrecan exhibited longer core protein length, longer CS-GAG length, and denser packing of CS-GAGs, contributing to much stronger compression resistance (Fig. 5.4a, right panel). Taken together, these results provide direct molecular-level evidence about the effects of age on cartilage matrix changes, which may assist the intervention of age-associated cartilage degeneration and OA initiation.

Despite being part of the natural homeostatic process, aggrecan fragmentation is more aggravated during the initiation of OA. Inspired by the molecular-level studies by Grodzinsky, Chery et al. investigated how aggrecan degeneration alters the micromechanics of pericellular matrix (PCM), the immediate microenvironment of chondrocytes, and in turn, the mechanotransduction of chondrocytes in post-traumatic OA. In the destabilization of the medial meniscus (DMM) murine model [18], the micromodulus of PCM was measured by immunofluorescence (IF)-guided AFM nanomechanical mapping (Fig. 5.4b), and was found to show significant reduction as early as 3 days post-surgery relative to the Sham control. This reduction preceded both changes of overt tissue-level mechanical properties measured by classical AFM-nanoindentation (1 week after) [13], and appearance of histological cartilage damage (4–8 weeks after) [18]. This weakening of the PCM can be attributed to accelerated aggrecan degradation in OA, as the aggrecan neo-epitopes (e.g., VDIPEN) were found to be mainly localized in the pericellular domain at this early stage. In alignment with the PCM degeneration, at 3 days after DMM, chondrocytes also exhibited

demoted intracellular calcium signaling, $[Ca^{2+}]_i$, activities, one of the earliest, fundamental cell responses to mechanical stimuli [8]. This effect was most pronounced under hypo-osmotic stimuli, which simulate the amplified GAG-GAG EDL repulsion and increased cell strain during compressive joint loading. Conversely, when the aggravated catabolism was attenuated by small molecule inhibitor, GM6001, the reduction of PCM modulus and disruption of $[Ca^{2+}]_i$ activities could be effectively rescued. Thus, aggravated aggrecan degradation represents a key molecular event in the initiation of OA, which not only impacts the tissue-level mechanical properties, but disrupts chondrocyte mechanotransduction by impairing the PCM.

Understanding the molecular aspects of aggrecan in normal aging and disease initiation also shed light on the development of novel tissue engineering and regeneration strategies. In tissue engineering, the use of primary chondrocytes is challenged by the limited amount of cells and donor site morbidity. Bone marrow stromal cells (BMSCs) are often used as the alternative cell source [41]. When undergoing chondrogenesis, BMSCs were found to synthesize full length aggrecan within 1–2 weeks of chondrogenic culture [33, 37]. Adult equine BMSCs undergoing chondrogenesis within hydrogel cultures could synthesize aggrecan molecules having CS-GAG chains that were almost 2× longer than the CS-GAGs synthesized by primary chondrocytes harvested from those same horses (Fig. 5.4c). Importantly, it was also discovered via fluorophore-assisted carbohydrate electrophoresis (FACE) analysis that the aggrecan made by these adult BMSCs demonstrated CS-GAG sulfation patterns typical of those observed in newborn growth cartilage, even though these cells were originated from adult animals. The BMSC-derived aggrecan also showed higher compressive stiffness, close to that of newborn human aggrecan as seen in Fig. 5.4a. On the other hand, in comparison to primary chondrocytes, BMSCs had a lower synthesis rate of collagen and proteoglycans, as well as a lower retention rate of newly synthesized aggrecan in its neo-matrix. This resulted in a lesser assembled matrix with lower sGAG content in the BMSC neo-matrix [1]. When assessed via AFM-nanorheometer, BMSC neo-matrix showed a higher degree of energy dissipation and similar elastic modulus at lower frequencies, but lower modulus at high frequency relative to that of chondrocyte neo-matrix [34, 35]. Therefore, despite its capability of synthesizing more superior aggrecan, BMSCs may also have inferior capabilities in biosynthesis and neo-matrix assembly. These factors need to be considered and modulated at both molecular and cellular levels to enhance the quality of regenerative tissues.

5.4 Other Native and Biomimetic Proteoglycans

In addition to aggrecan, cartilage matrix also consists of many other proteoglycans and glycoproteins, including small leucine rich proteoglycans (SLRPs), perlecan, lubricin, matrilins and cartilage oligomeric matrix protein (COMP) [28]. These molecules are present at minor quantities, and thus, do not directly contribute to tissue biomechanics. However, they could have important roles in regulating matrix assembly or cell-matrix interactions through specific interactions with other matrix molecules, cell surface receptors, and/or cytokines [32]. Regulatory roles of individual proteoglycans have been studied by assessing the phenotype of various genetic knockout murine models [28]. Previously, analysis of murine cartilage phenotype has been mainly limited to gross-level assays, such as bulk chemistry, histology, immunohistochemistry, and micro-computed tomography (μCT). Assessment of the functional relevance of these molecules was challenged by the small volume and irregular shape of murine cartilage, which renders conventional biomechanical tools not applicable.

The nanomechanical paradigm established by Grodzinsky and colleagues enabled direct quantification of murine cartilage biomechanical properties, providing a new path for pinpointing the activities of individual proteoglycans [22]. For example, a recent study by Han et al. investigated the role of decorin in cartilage biomechanical function and OA progression [21]. Decorin is a class I SLRP containing ~40 kDa leucine rich

core protein with one CS- or dermatan sulfate (DS)-GAG chain attached near its N-terminal. In human cartilage, the concentration of decorin is ≈ 15 nmol/ml, comparable to that of aggrecan (≈ 20 nmol/ml) [47], which implies its potential importance to cartilage integrity. In both decorin-null (*Dcn*$^{-/-}$) and inducible decorin knockout mice (*Dcn*$^{f/f}$/*Rosa26Cre*^{ER}, or *Dcn*^{iKO}), loss of decorin resulted in reduced aggrecan and sGAG content in the ECM (Fig. 5.5a). When tested under the AFM-nanorheometer, decorin-deficient cartilage demonstrated compromised biomechanical properties, including lower modulus, higher hydraulic permeability and reduced fluid pressurization (Fig. 5.5b, c). These observations highlighted a crucial role of decorin in regulating the integrity of aggrecan in cartilage ECM. This hypothesis was supported by molecular-level

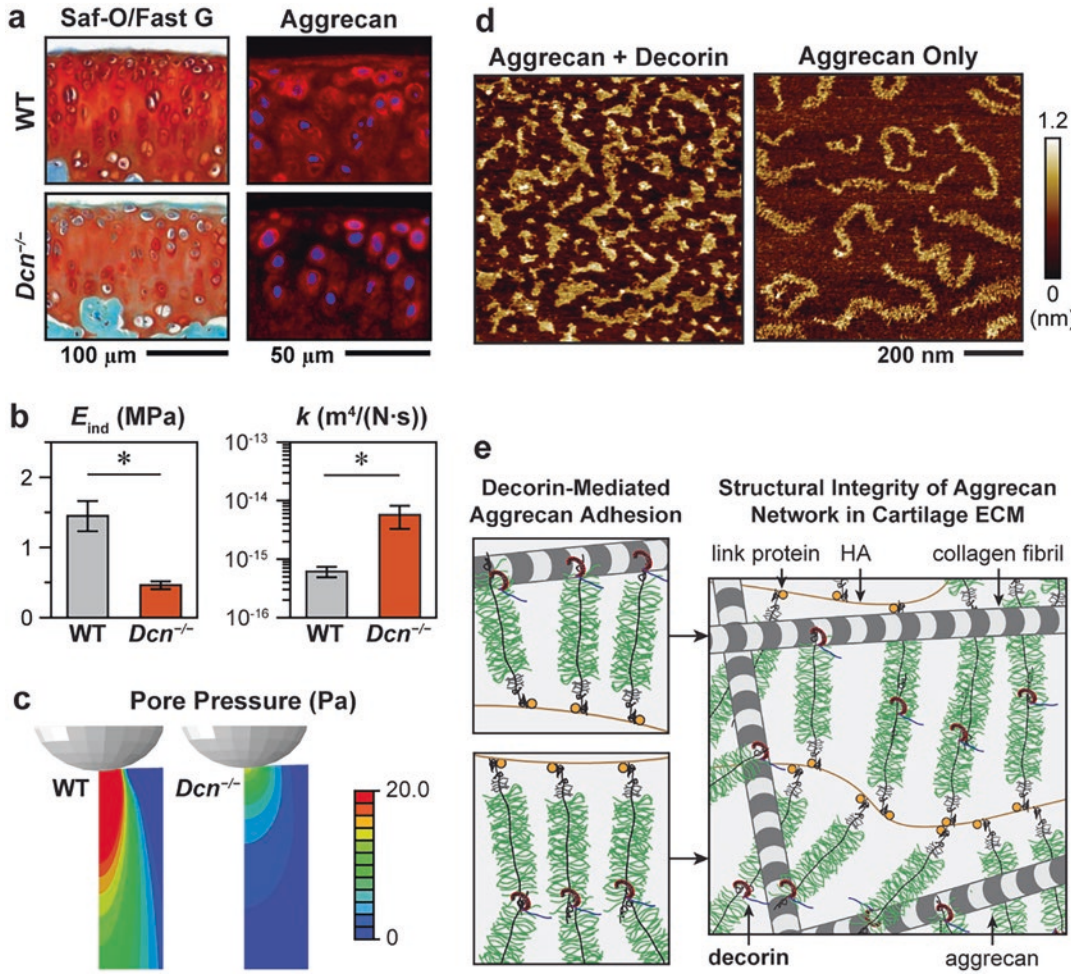

Fig. 5.5 Decorin regulates the integrity of aggrecan and biomechanics of cartilage ECM. a-c) Structural and biomechanical phenotype of *Dcn*$^{-/-}$ murine cartilage relative to the wild-type (WT) control at 3 months of age. (**a**) Safranin-O/Fast Green histology and IF images show the reduction of sulfated glycoaminoglycans (sGAGs) and aggrecan in *Dcn*$^{-/-}$ cartilage. (**b**) AFM-based nanoindentation and nanorheometric tests show the reduction of indentation modulus, E_{ind}, and the increase of hydraulic permeability, k, of cartilage. (**c**) Maximum pore pressure calculated from the fibril-reinforced poroelastic finite element model at the peak frequency (~10 Hz) corresponding to maximum phase angle. (**d**) Tapping mode AFM height imaging shows the formation of interconnected supramolecular network when aggrecan is reconstituted with free decorin protein, and individual aggrecan monomers when reconstituted without. (**e**) Schematic illustration of the structural role of decorin in regulating the molecular adhesion of aggrecan-aggrecan and aggrecan-collagen fibrils, and thus, the integrity of cartilage ECM. (Panels (**a**)–(**e**) are adapted with permission from Ref. [21])

nanomechanical experiments. First, when free decorin protein was added to the solution, molecular adhesions between two opposing aggrecan layers, and between aggrecan and collagen II fibrils, were both significantly increased. Second, when decorin protein and aggrecan monomers were reconstituted on a mica surface, they formed interconnected supramolecular networks, despite the presence of strong EDL repulsion (Fig. 5.5d). These results corroborate the observation that *Dcn*$^{-/-}$ chondrocytes synthesized a similar amount of sGAGs, but a lesser portion was retained in the neo-matrix. Therefore, in cartilage, decorin could serve as a "physical linker", which in turn, strengthens the aggrecan-aggrecan and aggrecan-collagen II molecular adhesion, enhancing the integration of aggrecan network in cartilage (Fig. 5.5e) [21].

The impact of decorin on aggrecan integrity also regulates chondrocyte mechanotransduction. Applying immunofluorescence (IF)-guided AFM, Chery et al. showed that the PCM of *Dcn*$^{-/-}$ cartilage was impaired during post-natal growth, leading to demoted chondrocyte intracellular calcium signaling, $[Ca^{2+}]_i$, activities in situ [7]. This study further confirmed that such impairment can be attributed to the reduction of aggrecan and sGAG content in the PCM, supporting the role of decorin in mediating chondrocyte mechanobiology through regulating the integrity of aggrecan in the PCM. In the DMM model, both *Dcn*$^{-/-}$ and *Dcn*^{iKO} mice exhibited accelerated loss of sGAGs and fibrillation of cartilage surface, contributing to more severe OA relative to the control [38]. The mediation of aggrecan assembly was also found to be specific to decorin. Biglycan is another class I SLRP, whose core protein has ~57% structural homology to that of decorin, but harbors two, rather than one, CS/DS-GAG side chains near its N-terminal [30]. In contrast, such aggravated OA was not detected in biglycan inducible knockout mice (*Bgn*^{fff}*/Rosa26Cre*^{ER}) subjected to DMM surgery [20]. Therefore, building on the foundation established by Grodzinsky, these recent studies highlighted an indispensable role of decorin in regulating the integrity of aggrecan network in cartilage matrix, and thus, the ECM biomechanics and chondrocyte mechanotransduction. Meanwhile, decorin also contributes to the slow-down of OA progression by attenuating the loss of fragmented aggrecan and inhibiting cartilage fibrillation.

Besides decorin, the impact of perlecan on cartilage development and homeostasis has also been studied from the nanomechanics perspective. Perlecan is a basement membrane-specific heparan sulfate proteoglycan (HSPG, M_w ~ 470 kDa), and contains three heparan sulfate (HS)-GAG or CS-GAG chains near its N-terminal. In cartilage, perlecan is localized in the PCM, and is suggested to interact with collagens VI and XI to stabilize the matrix compartment [62]. It also directly regulates cell surface mechanosensing [19] and activation of fibroblast growth factor-2 (FGF-2) [57]. Applying IF-guided AFM, Wilusz et al. demonstrated direct contribution of perlecan and its HS-GAGs to PCM integrity. Heparinase III digestion was shown to increase the micromodulus of porcine cartilage PCM, but not that of the bulk ECM [61]. It was hypothesized that the HS-GAG chain of perlecan could contribute to the local fixed charges and osmotic swelling pressure, while its enzymatic removal may reduce the swelling of PCM and in turn, increase the apparent local modulus. Furthermore, in newborn perlecan knockdown mice (*Hspg2*$^{+/-}$), Xu et al. observed reduced cartilage matrix stiffness as well as defective PCM formation. Production of an abundance of matrix proteins was elevated, including atypical sGAGs, which was hypothesized to compensate for the loss of perlecan, illustrating an important role of perlecan in mediating initial matrix assembly [63].

Marcolongo and colleagues synthesized a family of biomimetic proteoglycans (BPGs) to recapitulate the biophysical characteristics of native aggrecan at the molecular level [48]. Specifically, BPG10 is a synthetic polymer consisting of a ~ 10 kDa synthetic poly(acrylic acid) (PAA) core, decorated with ~5–7 CS-GAG bristles (Fig. 5.6a). Similar to that of aggrecan, BPG10 exhibits the "bottle-brush" architecture, with CS-GAGs packed at 3–4 nm spacing along the PAA core [48], comparable to the 2–3 nm spacing of CS-GAGs along aggrecan core protein [43]. When infiltrated into bovine cartilage

explants, these BPGs were able to localize in the PCM and territorial domain [46] (Fig. 5.6b). Kahle et al. applied IF-guided AFM to BPG10-augmented bovine cartilage explant, and showed that its localization increased the micromodulus of PCM without altering properties of the matrix bulk (Fig. 5.6c) [31]. Such effect was attributed to the increased fixed charge density within the

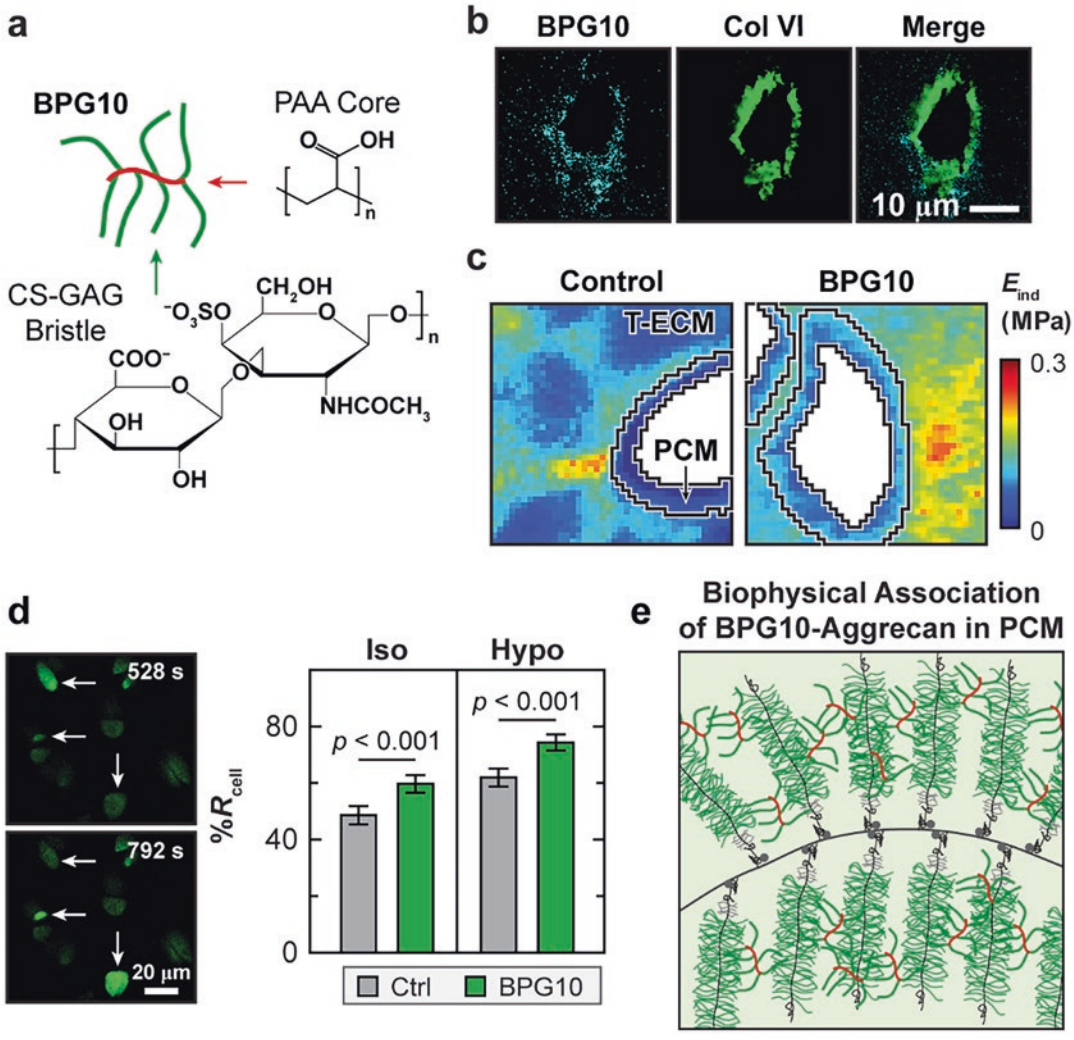

Fig. 5.6 Biomimetic proteoglycan, BPG10, strengthens cartilage pericellular matrix (PCM) and modulates chondrocyte mechanotransduction through integrating with the aggrecan network in the PCM. (**a**) BPG10 is synthesized by grafting natural chondroitin sulfate glycosaminoglycan (CS-GAG) bristles to an enzymatically resistant, synthetic poly (acrylic acid) (PAA) core. (**b**) IF images of adult bovine cartilage explants infiltrated with fluorescently-labeled BPG10 and co-stained with collagen VI demonstrate the preferred distribution of BPG10 within the PCM and nearby territorial domain. (**c**) Representative indentation modulus, E_{ind}, maps of control and BPG10-treated cartilage in 20 × 20 μm^2 regions of interest (ROIs) containing well-defined PCM rings (40 × 40 indents) via IF-guided AFM nanomechanical mapping illustrate the increase of PCM micromodulus by the infiltration of BPG10. (**d**) Left panel: Representative IF images of intracellular calcium signaling, $[Ca^{2+}]_i$, of adult bovine chondrocytes in situ. BPG10 enhances mechanosensing of chondrocytes in both isotonic and hypotonic (osmotically-simulated compression) conditions, as illustrated by an increase in the percentage of responding cells, $\%R_{cell}$ (mean ± 95% CI, ≥ 445 cells from n = 3 animals). (**e**) Schematic illustration of biophysical adhesion interactions between BPG10 and aggrecan, which enables the integration of BPG10 with the aggrecan-enriched cartilage PCM, and thus, the preferred localization of BPG10 in the PCM. (Panels (**a**)–(**e**) are adapted with permission from Ref. [31])

PCM due to the localization of BPG10. In turn, residing chondrocytes in BPG10-augmented PCM exhibited enhanced *in situ* $[Ca^{2+}]_i$ activities (Fig. 5.6d). When tested by molecular force spectroscopy, these BPG10 molecules demonstrated the capability of undergoing molecular adhesion with other BPG10 molecules and with native aggrecan, at a similar adhesion magnitude as aggrecan-aggrecan self-adhesion. Thus, it was hypothesized that by mimicking the "brush-like" ultrastructure and polyanionic nature of aggrecan, BPG10 can integrate with aggrecan in native cartilage through biophysical adhesions (Fig. 5.6e), and thus, has the potential to be used for harnessing cell mechanoresponses and modifying disease progression [31].

5.5 Summary and Outlook

This chapter summarized the transformative impact of Dr. Grodzinsky's contributions to the understanding of aggrecan molecular mechanics at the nanoscale. By developing and applying an array of AFM-based nanomechanical modalities to cartilage molecules, cells, and tissues, this body of work established a new front in understanding the origins of cartilage ECM functions, cell-ECM interactions, and disease initiation events. In addition, as discussed in this chapter, this nanotechnology paradigm established by Dr. Grodzinsky opened the door for further in-depth studies on the roles of other minor proteoglycans and proteins in cartilage biomechanics and mechanobiology, as well as the evaluation of novel molecular therapeutic strategies for OA treatment. It is expected that many future studies will benefit immensely from this molecular foundation established by Dr. Grodzinsky, which is one of the many fronts that he has contributed in musculoskeletal research.

Acknowledgements The authors would like to thank Alan J. Grodzinsky for his mentorship, inspiration and invaluable support over the past decades. We would also like to acknowledge the support from National Science Foundation Grant CMMI-1751898 and National Institutes of Health Grant AR074490.

References

1. Babalola OM, Bonassar LJ (2010) Effects of seeding density on proteoglycan assembly of passaged mesenchymal stem cells. Cell Mol Bioeng 3:197–206
2. Biot MA (1956) Theory of propagation of elastic waves in a fluid-saturated porous solid. I Low-frequency range. J Acoust Soc Am 28:168–178
3. Buckwalter JA, Rosenberg L (1983) Structural changes during development in bovine fetal epiphyseal cartilage. Coll Relat Res 3:489–504
4. Buckwalter JA, Rosenberg LC, Tang L-H (1984) The effect of link protein on proteoglycan aggregate structure – an electron microscopic study of the molecular architecture and dimensions of proteoglycan aggregates reassembled from the proteoglycan monomers and link proteins of bovine fetal epiphyseal cartilage. J Biol Chem 259:5361–5363
5. Buschmann MD, Grodzinsky AJ (1995) A molecular model of proteoglycan-associated electrostatic forces in cartilage mechanics. J Biomech Eng 117:179–192
6. Chery DR, Han B, Li Q, Zhou Y, Heo SJ, Kwok B, Chandrasekaran P, Wang C, Qin L, Lu XL, Kong D, Enomoto-Iwamoto M, Mauck RL, Han L (2020) Early changes in cartilage pericellular matrix micromechanobiology portend the onset of post-traumatic osteoarthritis. Acta Biomater 111:267–278
7. Chery DR, Han B, Zhou Y, Wang C, Adams SM, Chandrasekaran P, Kwok B, Heo SJ, Enomoto-Iwamoto M, Lu XL, Kong D, Iozzo RV, Birk DE, Mauck RL, Han L (2021) Decorin regulates cartilage pericellular matrix micromechanobiology. Matrix Biol 96:1–17
8. Clapham DE (2007) Calcium signaling. Cell 131:1047–1058
9. Clark IC (1971) Articular cartilage: a review and scanning electron microscopy study. I The interterritorial fibrillar architecture. J Bone Joint Surg Br 53B:732–750
10. Dean D, Han L, Grodzinsky AJ, Ortiz C (2006) Compressive nanomechanics of opposing aggrecan macromolecules. J Biomech 39:2555–2565
11. Dean D, Han L, Ortiz C, Grodzinsky AJ (2005) Nanoscale conformation and compressibility of cartilage aggrecan using microcontact printing and atomic force microscopy. Macromolecules 38:4047–4049
12. Dean D, Seog J, Ortiz C, Grodzinsky AJ (2003) Molecular-level theoretical model for electrostatic interactions within polyelectrolyte brushes: applications to charged glycosaminoglycans. Langmuir 19:5526–5539
13. Doyran B, Tong W, Li Q, Jia H, Zhang X, Chen C, Enomoto-Iwamoto M, Lu XL, Qin L, Han L (2017) Nanoindentation modulus of murine cartilage: a sensitive indicator of the initiation and progression of post-traumatic osteoarthritis. Osteoarthr Cartil 25:108–117

14. Eisenberg SR, Grodzinsky AJ (1988) Electrokinetic micromodel of extracellular matrix and other polyelectrolyte networks. Physicochem Hydrodyn 10:517–539
15. Eyre DR, Weis MA, Wu J-J (2006) Articular cartilage collagen: an irreplaceable framework? Eur Cell Mater 12:57–63
16. Frank EH, Grodzinsky AJ (1987a) Cartilage electromechanics – I. Electrokinetic transduction and the effects of electrolyte pH and ionic strength. J Biomech 20:615–627
17. Frank EH, Grodzinsky AJ (1987b) Cartilage electromechanics – II. A continuum model of cartilage electrokinetics and correlation with experiments. J Biomech 20:629–639
18. Glasson SS, Blanchet TJ, Morris EA (2007) The surgical destabilization of the medial meniscus (DMM) model of osteoarthritis in the 129/SvEv mouse. Osteoarthr Cartil 15:1061–1069
19. Gubbiotti MA, Neill T, Iozzo RV (2017) A current view of perlecan in physiology and pathology: a mosaic of functions. Matrix Biol 57–58:285–298
20. Han B, Li Q, Wang C, Chandrasekaran P, Zhou Y, Qin L, Liu XS, Enomoto-Iwamoto M, Kong D, Iozzo RV, Birk DE, Han L (2021) Differentiated activities of decorin and biglycan in the progression of post-traumatic osteoarthritis. Osteoarthr Cartil 29:1181–1192
21. Han B, Li Q, Wang C, Patel P, Adams SM, Doyran B, Nia HT, Oftadeh R, Zhou S, Li CY, Liu XS, Lu XL, Enomoto-Iwamoto M, Qin L, Mauck RL, Iozzo RV, Birk DE, Han L (2019) Decorin regulates the aggrecan network integrity and biomechanical functions of cartilage extracellular matrix. ACS Nano 13:11320–11333
22. Han B, Nia HT, Wang C, Chandrasekaran P, Li Q, Chery DR, Li H, Grodzinsky AJ, Han L (2017) AFM-nanomechanical test: an interdisciplinary tool that links the understanding of cartilage and meniscus biomechanics, osteoarthritis degeneration and tissue engineering. ACS Biomater Sci Eng 3:2033–2049
23. Han L, Dean D, Daher LA, Grodzinsky AJ, Ortiz C (2008) Cartilage aggrecan can undergo self-adhesion. Biophys J 95:4862–4870
24. Han L, Dean D, Mao P, Ortiz C, Grodzinsky AJ (2007a) Nanoscale shear deformation mechanisms of opposing cartilage aggrecan macromolecules. Biophys J 93:L23–L25
25. Han L, Dean D, Ortiz C, Grodzinsky AJ (2007b) Lateral nanomechanics of cartilage aggrecan macromolecules. Biophys J 92:1384–1398
26. Han L, Grodzinsky AJ, Ortiz C (2011) Nanomechanics of the cartilage extracellular matrix. Annu Rev Mater Res 41:133–168
27. Hardingham TE, Muir H (1972) The specific interaction of hyaluronic acid with cartilage proteoglycans. Biochim Biophys Acta 279:401–405
28. Heinegård D (2009) Proteoglycans and more – from molecules to biology. Int J Exp Pathol 90:575–586
29. Huey DJ, Athanasiou KA (2011) Maturational growth of self-assembled, functional menisci as a result of TGF-beta 1 and enzymatic chondroitinase-ABC stimulation. Biomaterials 32:2052–2058
30. Iozzo RV (1998) Matrix proteoglycans: from molecular design to cellular function. Annu Rev Biochem 67:609–652
31. Kahle ER, Han B, Chandrasekaran P, Phillips ER, Mulcahey MK, Lu XL, Marcolongo MS, Han L (2022) Molecular engineering of pericellular microniche via biomimetic proteoglycans modulates cell mechanobiology. ACS Nano 16:1220–1230
32. Karamanos NK, Piperigkou Z, Theocharis AD, Watanabe H, Franchi M, Baud S, Brézillon S, Götte M, Passi A, Vigetti D, Ricard-Blum S, Sanderson RD, Neill T, Iozzo RV (2018) Proteoglycan chemical diversity drives multifunctional cell regulation and therapeutics. Chem Rev 118:9152–9232
33. Kopesky PW, Lee H-Y, Vanderploeg EJ, Kisiday JD, Frisbie DD, Plaas AHK, Ortiz C, Grodzinsky AJ (2010) Adult equine bone marrow stromal cells produce a cartilage-like ECM mechanically superior to animal-matched adult chondrocytes. Matrix Biol 29:427–438
34. Lee B, Han L, Frank EH, Chubinskaya S, Ortiz C, Grodzinsky AJ (2010a) Dynamic mechanical properties of the tissue-engineered matrix associated with individual chondrocytes. J Biomech 43:469–476
35. Lee B, Han L, Frank EH, Grodzinsky AJ, Ortiz C (2015) Dynamic nanomechanics of individual bone marrow stromal cells and cell-matrix composites during chondrogenic differentiation. J Biomech 48:171–175
36. Lee H-Y, Han L, Roughley PJ, Grodzinsky AJ, Ortiz C (2013) Age-related nanostructural and nanomechanical changes of individual human cartilage aggrecan monomers and their glycosaminoglycan side chains. J Struct Biol 181:264–273
37. Lee H-Y, Kopesky PW, Plaas AHK, Sandy JD, Kisiday J, Frisbie D, Grodzinsky AJ, Ortiz C (2010b) Adult bone marrow stromal cell-based tissue-engineered aggrecan exhibits ultrastructure and nanomechanical properties superior to native cartilage. Osteoarthr Cartil 18:1477–1486
38. Li Q, Han B, Wang C, Tong W, Wei Y, Tseng WJ, Han LH, Liu XS, Enomoto-Iwamoto M, Mauck RL, Qin L, Iozzo RV, Birk DE, Han L (2020) Mediation of cartilage matrix degeneration and fibrillation by decorin in post-traumatic osteoarthritis. Arthritis Rheumatol 72:1266–1277
39. Lu XL, Mow VC (2008) Biomechanics of articular cartilage and determination of material properties. Med Sci Sports Exerc 40:193–199
40. Maroudas A (1979) Physicochemical properties of articular cartilage. In: Freeman MAR (ed) Adult Articular Cartilage. Pitman, Tunbridge Wells, pp 215–290
41. Mauck RL, Yuan X, Tuan RS (2006) Chondrogenic differentiation and functional maturation of bovine mesenchymal stem cells in long-term agarose culture. Osteoarthr Cartil 14:179–189

42. Mow VC, Kuei SC, Lai WM, Armstrong CG (1980) Biphasic creep and stress relaxation of articular cartilage in compression: theory and experiments. J Biomech Eng 102:73–84
43. Ng L, Grodzinsky AJ, Patwari P, Sandy J, Plaas A, Ortiz C (2003) Individual cartilage aggrecan macromolecules and their constituent glycosaminoglycans visualized via atomic force microscopy. J Struct Biol 143:242–257
44. Nia HT, Han L, Bozchalooi IS, Roughley P, Youcef-Toumi K, Grodzinsky AJ, Ortiz C (2015) Aggrecan nanoscale solid-fluid interactions are a primary determinant of cartilage dynamic mechanical properties. ACS Nano 9:2614–2625
45. Pearle AD, Warren RF, Rodeo SA (2005) Basic science of articular cartilage and osteoarthritis. Clin Sports Med 24:1–12
46. Phillips ER, Haislup BD, Bertha N, Lefchak M, Sincavage J, Prudnikova K, Shallop B, Mulcahey MK, Marcolongo MS (2019) Biomimetic proteoglycans diffuse throughout articular cartilage and localize within the pericellular matrix. J Biomed Mater Res A 107:1977–1987
47. Poole AR, Rosenberg LC, Reiner A, Ionescu M, Bogoch E, Roughley PJ (1996) Contents and distributions of the proteoglycans decorin and biglycan in normal and osteoarthritic human articular cartilage. J Orthop Res 14:681–689
48. Prudnikova K, Yucha RW, Patel P, Kriete AS, Han L, Penn LS, Marcolongo MS (2017) Biomimetic proteoglycans mimic macromolecular architecture and water uptake of natural proteoglycans. Biomacromolecules 18:1713–1723
49. Rojas FP, Batista MA, Lindburg CA, Dean D, Grodzinsky AJ, Ortiz C, Han L (2014) Molecular adhesion between cartilage extracellular matrix macromolecules. Biomacromolecules 15:772–780
50. Sandy JD, Flannery CR, Neame PJ, Lohmander LS (1992) The structure of aggrecan fragments in human synovial fluid. Evidence for the involvement in osteoarthritis of a novel proteinase which cleaves the Glu 373-Ala 374 bond of the interglobular domain. J Clin Invest 89:1512–1516
51. Seog J, Dean D, Plaas AHK, Wong-Palms S, Grodzinsky AJ, Ortiz C (2002) Direct measurement of glycosaminoglycan intermolecular interactions via high-resolution force spectroscopy. Macromolecules 35:5601–5615
52. Seog J, Dean D, Rolauffs B, Wu T, Genzer J, Plaas AHK, Grodzinsky AJ, Ortiz C (2005) Nanomechanics of opposing glycosaminoglycan macromolecules. J Biomech 38:1789–1797
53. Seog J, Dean DM, Frank EH, Ortiz C, Grodzinsky AJ (2004) Preparation of end-grafted polyelectrolytes on nanoscale probe tips using an electric field. Macromolecules 37:1156–1158
54. Soltz MA, Ateshian GA (2000) A conewise linear elasticity mixture model for the analysis of tension-compression nonlinearity in articular cartilage. J Biomech Eng 122:576–586
55. Soulhat J, Buschmann MD, Shirazi-Adl A (1999) A fibril-network-reinforced biphasic model of cartilage in unconfined compression. J Biomech Eng 121:340–347
56. Vanden Berg-Foels WS, Scipioni L, Huynh C, Wen X (2012) Helium ion microscopy for high-resolution visualization of the articular cartilage collagen network. J Microsc 246:168–176
57. Vincent TL, McLean CJ, Full LE, Peston D, Saklatvala J (2007) FGF-2 is bound to perlecan in the pericellular matrix of articular cartilage, where it acts as a chondrocyte mechanotransducer. Osteoarthr Cartil 15:752–763
58. Wang C, Brisson BK, Terajima M, Li Q, Hoxha K, Han B, Goldberg AM, Sherry Liu X, Marcolongo MS, Enomoto-Iwamoto M, Yamauchi M, Volk SW, Han L (2020) Type III collagen is a key regulator of the collagen fibrillar structure and biomechanics of articular cartilage and meniscus. Matrix Biol 85–86:47–67
59. Wight TN, Heinegård DK, Hascall VC (1991) Cell biology of extracellular matrix. Plenum press, New York
60. Williamson AK, Chen AC, Sah RL (2001) Compressive properties and function-composition relationships of developing bovine articular cartilage. J Orthop Res 19:1113–1121
61. Wilusz RE, Defrate LE, Guilak F (2012) A biomechanical role for perlecan in the pericellular matrix of articular cartilage. Matrix Biol 31:320–327
62. Wilusz RE, Sanchez-Adams J, Guilak F (2014) The structure and function of the pericellular matrix of articular cartilage. Matrix Biol 39:25–32
63. Xu X, Li Z, Leng Y, Neu CP, Calve S (2016) Knockdown of the pericellular matrix molecule perlecan lowers in situ cell and matrix stiffness in developing cartilage. Dev Biol 418:242–247